A homogenization approach to the ultimate strength of brick masonry

Patrick de Buhan, Gianmarco de Felice

▶ **To cite this version:**

Patrick de Buhan, Gianmarco de Felice. A homogenization approach to the ultimate strength of brick masonry. Journal of the Mechanics and Physics of Solids, 1997, 45, pp.1085-1104. 10.1016/S0022-5096(97)00002-1 . hal-00111570

HAL Id: hal-00111570
https://hal.science/hal-00111570

Submitted on 20 Apr 2024

HAL is a multi-disciplinary open access archive for the deposit and dissemination of scientific research documents, whether they are published or not. The documents may come from teaching and research institutions in France or abroad, or from public or private research centers.

L'archive ouverte pluridisciplinaire **HAL**, est destinée au dépôt et à la diffusion de documents scientifiques de niveau recherche, publiés ou non, émanant des établissements d'enseignement et de recherche français ou étrangers, des laboratoires publics ou privés.

A homogenization approach to the ultimate strength of brick masonry

Patrick de Buhan[a] and Gianmarco de Felice[b]

[a]Laboratoire de Mécanique des Solides, ENPC-CERCSO. 6 et 8 av. B. Pascal, Marne-la-Vallée, France
[b]Dipartimento di Progettazione e Scienze dell'Architettura. Universita degli studi Roma Tre. Rome. Italy

A continuum model for assessing the ultimate failure of masonry as a homogenized material is presented in this paper. It is shown in particular how a homogenization technique implemented within the framework of the yield design theory, makes it possible to construct a macroscopic strength criterion for masonry described as a regular assemblage of bricks separated by joint interfaces. Making use of the kinematic definition of such a criterion which involves velocity jumps across the joints, the yield strength domain in the space of stresses is explicitly determined in the case of infinitely resistant bricks. It clearly shows the anisotropic characteristics of the equivalent medium, due to the preferential orientations of joints. This formulation is particularly interesting from an engineering point of view, since only a few easy to identify parameters relating to the joint strength characteristics (reduced here to a friction angle and a cohesion), and to the brick geometry are involved. As an illustrative application of the criterion so obtained, the stability of masonry walls subjected to inclined gravity loads is investigated by means of the upper-bound kinematic approach. Even though the theoretical predictions derived from this analysis are in good qualitative agreement with available experimental data, the comparison points to the necessary extension of such an approach for taking "scale effects" into account.

Keywords: B. anisotropic material, B. friction, C. linear programming, C. homogenization.

1. INTRODUCTION

At first glance traditional masonry may be regarded as a heterogeneous medium made of regularly arranged discrete blocks separated by joints. Early attempts to model joints by means of interface elements date back to Page (1978). At the same time limit analysis methods were employed to analyse the stability of such an assemblage of blocks in unilateral and frictional contact (Livesley, 1978). The approach was quite similar to the discrete element method proposed by Cundall (1971) in the field of rock mechanics and recently applied by Guiffrè *et al.* (1994) for the design of masonry walls. Other authors have proposed to model the behaviour of joints by a set of nonlinear shear and normal springs (Baggio and Trovalusci, 1993), while the blocks themselves were treated as elastic or rigid bodies. More elaborated constitutive models for joint interfaces have been developed recently by Lofti and Shing (1994) in order to account for dilatancy, the non-associated flow rule and softening behaviour.

All these approaches are based upon a simple idealization of masonry structures,

in which failure of joints is considered to play the decisive role in the nonlinear response of masonry as a whole. Whereas this model proves quite satisfactory for ancient stone masonry structures where mortar is either absent or no more effective (Heyman, 1966), its validity might be questioned for brickwork where it only partially accounts for the brick–mortar interaction. Furthermore, such models can hardly be used in practice for structural design, since they require a separate discretization of bricks and joints, leading to intractable numerical difficulties as the size of the problem increases. A continuum model in which the masonry is regarded as a homogeneous but obviously anisotropic material seems far more preferable in this case.

Several attempts have already been made to derive the mechanical properties of masonry as a homogenized material through micromechanics considerations. Pande *et al.* (1989), for instance, have deduced equivalent elastic moduli of brick masonry from the elastic properties of its individual components. Relying upon simplifying assumptions concerning the geometry of the microstructure, as well as the relationship between microscopic and macroscopic quantities, some authors such as Maier *et al.* (1991) or Pietruszczack and Niu (1992) have succeeded in formulating nonlinear constitutive laws for the homogenized material. By resorting to the homogenization theory for periodic media, Anthoine (1995) proposed a numerical method for deriving the global elastic coefficients of masonry, taking into account the elasticity of both constituents (brick and mortar) as well as the finite thickness of the joints. Quite recently Alpa and Monetto (1994) have presented a comprehensive formulation for the constitutive behaviour of in-plane loaded dry block masonry walls, with special attention to failure analysis.

The present work is closely connected with the latter kind of analysis. It is based on the yield design homogenization method, which provides a rigorous theoretical framework for determining yield strength properties of periodic composite media from the local strength properties of their components. Previously developed for reinforced soils (de Buhan and Salençon, 1990), fibre composite materials (de Buhan and Taliercio, 1991) or jointed rock masses (Bekaert and Maghous, 1996), the method has been recently implemented by de Felice (1994) for the treatment of block masonry. As will be shown here, such an approach is readily applicable to the case where failure of the bricks themselves has also to be taken into account in the analysis.

2. FUNDAMENTALS OF THE HOMOGENIZATION METHOD FOR PERIODIC MEDIA

Consider a structure occupying a domain Ω, made up of a periodic heterogeneous material, in such a manner that it is possible to exhibit a "unit cell", denoted by A, which may be regarded as the smallest representative volume of material (Fig. 1). This means that A contains all information necessary to describe the structure completely.

For a given periodicity characterized by three vectors forming a base in the 3-D Euclidean space, it is always possible to select, as the unit cell, the parallelepipedic volume constructed from this base. It can be shown (Suquet, 1983; de Buhan, 1986) that the determination of the macroscopic strength condition of the above periodic

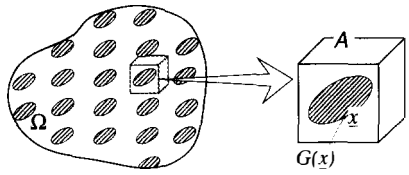

Fig. 1. Periodic heterogeneous material and representative unit cell.

heterogeneous material amounts to solving a yield design boundary value problem attached to the unit cell.

More precisely, introducing at every point $\underline{x}$ of A the convex domain $G(\underline{x})$ characterizing the strength capacities of the constituent material at this same point, one may define the macroscopic strength domain, denoted by G^{hom}, as the set of "macroscopic" stress states $\underline{\underline{\Sigma}}$ such that there exists a stress field $\underline{\underline{\sigma}}$ defined over A and verifying the following conditions:

$$\underline{\underline{\Sigma}} = \langle \underline{\underline{\sigma}}(\underline{x}) \rangle = \frac{1}{|A|} \int_A \underline{\underline{\sigma}}(\underline{x}) \, \mathrm{d}A, \tag{1a}$$

$$\operatorname{div} \underline{\underline{\sigma}}(\underline{x}) = \underline{0}, \tag{1b}$$

$\underline{\underline{\sigma}}(\underline{x}) \cdot \underline{n}(\underline{x})$ antiperiodic, i.e. taking opposite values on opposite sides of A,

$\underline{n}$ being the unit normal oriented outwards, (1c)

$$\underline{\underline{\sigma}}(\underline{x}) \in G(\underline{x}) \quad \text{whatever } \underline{x} \in A. \tag{1d}$$

Conditions (1a)–(1c) express that $\underline{\underline{\sigma}}$ is in equilibrium with $\underline{\underline{\Sigma}}$, while condition (1d) represents the strength requirement. They all constitute the static definition of G^{hom}.

A kinematic definition of G^{hom} can be obtained as follows through the dualization of the static definition by means of the principle of virtual work. Considering any virtual velocity field of the form

$$\underline{v}(\underline{x}) = \underline{\underline{F}} \cdot \underline{x} + \underline{u}(\underline{x}), \tag{2}$$

where $\underline{\underline{F}}$ represents any second order tensor and $\underline{u}$ is a periodic velocity field assumed first to be everywhere differentiable, the associated strain rate field $\underline{\underline{d}}$, defined as

$$\underline{\underline{d}}(\underline{x}) = \tfrac{1}{2}(\underline{\underline{\operatorname{grad} v}} + {}^{t}\underline{\underline{\operatorname{grad} v}})(\underline{x}) \tag{3}$$

can be written

$$\underline{\underline{d}}(\underline{x}) = \underline{\underline{D}} + \underline{\underline{\delta}}(\underline{x}), \tag{4}$$

where $\underline{\underline{D}}$ is the symmetric part of $\underline{\underline{F}}$ and $\underline{\underline{\delta}}$ is the strain rate field associated with $\underline{u}$.

Using the principle of virtual work, one may write

$$\int_A (\underline{\underline{\sigma}} : \underline{\underline{d}}) \, \mathrm{d}A = \int_{\partial A} (\underline{\underline{\sigma}} \cdot \underline{n}) \cdot \underline{v} \, \mathrm{d}S \tag{5}$$

for any stress field $\underline{\underline{\sigma}}$ verifying (1a)–(1c) and any virtual velocity field $\underline{v}$ of the form (2). The right hand member of (5) may be transformed into

$$\int_{\partial A} (\underline{\underline{\sigma}} \cdot \underline{n}) \cdot (\underline{\underline{F}} \cdot \underline{x}) \, \mathrm{d}S + \int_{\partial A} (\underline{\underline{\sigma}} \cdot \underline{n}) \cdot \underline{u} \, \mathrm{d}S,$$

where the second term vanishes, since $\underline{u}$ is periodic and $\underline{\underline{\sigma}} \cdot \underline{n}$ is antiperiodic. It follows that

$$\int_A (\underline{\underline{\sigma}} : \underline{\underline{d}}) \, \mathrm{d}A = \left(\int_A \underline{\underline{\sigma}} \, \mathrm{d}A \right) : \underline{\underline{F}}$$

or, introducing the notation

$$\langle \cdot \rangle = \frac{1}{|A|} \int_A \cdot \, \mathrm{d}A, \tag{6}$$

$$\langle \underline{\underline{\sigma}} : \underline{\underline{d}} \rangle = \underline{\underline{\Sigma}} : \underline{\underline{F}} = \underline{\underline{\Sigma}} : \underline{\underline{D}}.$$

Referring to the concept of loading mode of a mechanical system (see, e.g., Salençon, 1992), it is apparent from (6) that the boundary value problem defined over the unit cell corresponds to such a loading mode depending on a finite number of parameters, namely the six independent components of $\underline{\underline{\Sigma}}$. The generalized kinematic parameters which are associated with the load parameters by duality are the components of $\underline{\underline{D}}$. Introducing

$$\pi(\underline{\underline{d}}) = \max_{\underline{\underline{\sigma}}} \{ \underline{\underline{\sigma}} : \underline{\underline{d}} ; \underline{\underline{\sigma}} \in G(\underline{x}) \} \tag{7}$$

which is the support function of the convex domain $G(\underline{x})$, and

$$\pi^{\mathrm{hom}}(\underline{\underline{D}}) = \max_{\underline{\underline{\Sigma}}} \{ \underline{\underline{\Sigma}} : \underline{\underline{D}} ; \underline{\underline{\Sigma}} \in G^{\mathrm{hom}} \}, \tag{8}$$

it results, from the static definition (1) of G^{hom} and from (6), that

$$\pi^{\mathrm{hom}}(\underline{\underline{D}}) \leqslant \langle \pi(\underline{\underline{d}}) \rangle \tag{9}$$

for any periodic $\underline{u}$. Furthermore, it can be proved under certain mathematical conditions (see, e.g., Frémond and Friaà, 1982), which will be assumed to be satisfied in the sequel, that

$$\pi^{\mathrm{hom}}(\underline{\underline{D}}) = \min_{\underline{u}} \{ \langle \pi(\underline{\underline{d}}) \rangle \}. \tag{10}$$

The latter equation represents the kinematic definition of G^{hom}. It can be geometrically interpreted in the six-dimensional space of stress $\underline{\underline{\Sigma}}$ (Fig. 2) where, for a given $\underline{\underline{D}}$, minimizing the functional $\langle \pi(\underline{\underline{d}}) \rangle$, which is called the maximum resisting work, over the set of all periodic velocity fields $\underline{u}$, results in determining the plane tangent to the boundary of G^{hom} at a point where $\underline{\underline{D}}$ is an outer normal. It follows that exploring all the possible directions for $\underline{\underline{D}}$ makes it possible to construct G^{hom} as the convex envelope of such tangent planes.

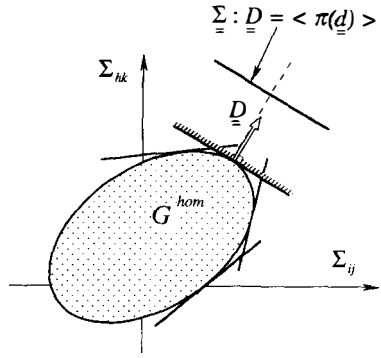

Fig. 2. Geometrical interpretation of the kinematic definition of G^{hom}.

3. MACROSCOPIC YIELD CRITERION FOR MASONRY

Consider a masonry structure, such as a panel made of rectangular bricks separated by horizontal continuous bed joints and alternate vertical head joints, subjected to in-plane loading. Figure 3 represents the corresponding diamond-shaped unit cell associated with the periodicity of the structure in the $0x_1x_2$ plane. Its vertices are located at the centres of four adjacent bricks as shown in the figure.

The strength capacities of the individual components of this composite material can be defined as follows:

- the brick material is assumed to be homogeneous obeying a "plane stress" failure condition characterized by a domain G^{b} in the three-dimensional stress space $(\sigma_{11}, \sigma_{12}, \sigma_{22})$;
- because their thickness may be considered as sufficiently small when compared with the brick dimensions, it seems quite reasonable to model the joints as (one-dimensional) interfaces; their failure condition, relating to the stress vector $\underline{T}$ acting upon those interfaces at any point, can be expressed by means of a convex function such as

$$g(\underline{T} = (\sigma, \tau)) \leqslant 0, \tag{11}$$

where σ and τ denote the normal and shear components of $\underline{T}$ respectively.

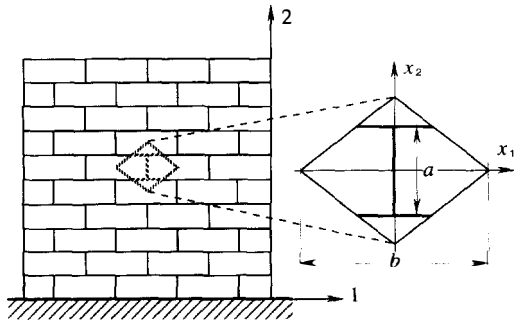

Fig. 3. Brick masonry structure and representative unit cell.

It is to be emphasized that no additional information regarding the constitutive behaviour of masonry components (bricks and joints) is required by the yield design approach which will be performed in the sequel. The results to be obtained do not depend on data such as the elastic stiffness characteristics, the initial state of stress prevailing in the unit cell prior to loading, or the loading path followed up to failure.

3.1. *Static definition of* G^{hom}

It is simply derived from the application of the general definition given by (1) that

$$G^{\text{hom}} = \{\underline{\underline{\Sigma}} = \langle \underline{\underline{\sigma}}(\underline{x}) \rangle, \underline{\underline{\sigma}}(\underline{x}) \cdot \underline{n}(\underline{x}) \quad \text{antiperiodic}, \operatorname{div} \underline{\underline{\sigma}}(\underline{x}) = \underline{0} \tag{12}$$

with

$$\underline{\underline{\sigma}}(\underline{x}) \in G^{\text{b}} \quad \forall \underline{x} \in A$$

and

$$g(\underline{\underline{\sigma}}(\underline{x}) \cdot \underline{n}(\underline{x})) \leqslant 0 \quad \forall \underline{x} \in J\},$$

where J denotes the set of joint segments of the cell and $\underline{n}(\underline{x})$ the unit normal at any point $\underline{x}$ of those segments.

3.2. *Kinematic definition of* G^{hom}

Owing to the existence of a failure condition defined by (11) along the joint interfaces, it becomes necessary to introduce a "π-function" similar to (7) so as to be able to perform the kinematic approach for determining G^{hom}. Such a function is defined as

$$\tilde{\pi}(\underline{n}; [\underline{v}]) = \max_{\underline{\underline{T}}} \{\underline{T} \cdot [\underline{v}]; g(\underline{T}) \leqslant 0\}, \tag{13}$$

where $[\underline{v}]$ denotes the velocity jump across the interface when following its normal $\underline{n}$. It is therefore essential to extend the kinematic approach by considering virtual velocity fields $\underline{v}$ involving discontinuities along the set of joints J belonging to the unit cell. Then the principle of virtual work expressed by (5) in the case of a continuous and differentiable velocity field, becomes

$$\int_{\partial A} (\underline{\underline{\sigma}} \cdot \underline{n}) \cdot \underline{v} \, \mathrm{d}S = \int_A (\underline{\underline{\sigma}} : \underline{\underline{d}}) \, \mathrm{d}A + \int_J \underline{T}(\underline{n}) \cdot [\underline{v}] \, \mathrm{d}J, \tag{14}$$

with $\underline{T}(\underline{n}) = \underline{\underline{\sigma}} \cdot \underline{n}$. The second integral in the right hand member of the above equation represents the contribution to the virtual work of deformation due to the discontinuities of $\underline{v}$ and hence of $\underline{u}$ across the joint interfaces. Consequently (10) remains valid, provided that the following extended definition of $\langle \pi(\underline{\underline{d}}) \rangle$ be adopted:

$$\langle \pi(\underline{\underline{d}}) \rangle = \frac{1}{|A|} \left(\int_A \pi(\underline{\underline{d}}) \, \mathrm{d}A + \int_J \tilde{\pi}(\underline{n}, [\underline{u}]) \, \mathrm{d}J \right). \tag{15}$$

4. APPLICATION TO BLOCK MASONRY

A particular, but nevertheless important case, which will be considered from now on, is that when the constituent material of the bricks forming the masonry structure may be considered as much more resistant than the joints. This assumption implies that the convex domain G^b amounts to the whole space R^3 of plane stresses. Moreover, the strength criterion of the joints will be particularized as being a Mohr–Coulomb strength condition:

$$g(\sigma, \tau) = |\tau| + \sigma \tan \varphi - c \leqslant 0, \tag{16}$$

where c denotes the cohesion and φ the friction angle.

4.1. *Kinematics of the unit cell*

The infinite strength assumption for the block material leads to an important simplification as regards the velocity fields to be employed in the yield design kinematic approach for determining G^{hom}. Indeed, as appears from (7) defining the π-function, in the case where $G(\underline{x}) = G^b = R^3$, $\pi(\underline{\underline{d}})$ takes infinite values for $\underline{\underline{d}} \neq \underline{\underline{0}}$. It follows that the only velocity fields that are worth considering (called relevant velocity fields), are those for which $\underline{\underline{d}} = \underline{\underline{0}}$ at every point of the block material, since any velocity field where the block material would deform virtually, would lead to an infinite value of $\langle \pi(\underline{\underline{d}}) \rangle$ and thus, referring to Fig. 2, to a plane going to infinity. Therefore, it is sufficient in the kinematic approach, to explore velocity fields whose restriction to each of the four blocks making up the unit cell, is a rigid body motion defined by

$$\underline{v}(\underline{x}) = \underline{v}^i + \omega^i \underline{e}_3 \wedge (\underline{x} - \underline{x}^i), \tag{17}$$

where $\underline{x}^i$ and $\underline{v}^i$ are respectively the position and the velocity of vertex A_i of the unit cell and ω^i denotes the angular velocity of block i ($i = 1$ to 4) (Fig. 4). Furthermore, the general form of kinematically admissible velocity fields expressed by (2), where $\underline{u}$ is periodic, imposes additional restrictions on the possible values of $\underline{v}^i$ and ω^i ($i = 1, \ldots, 4$), since, up to an arbitrary global rigid motion which can be disregarded, it is always possible to set

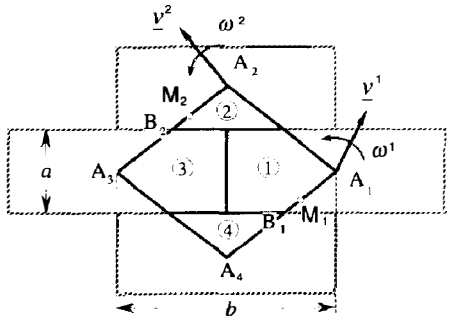

Fig. 4. Piecewise rigid block kinematics of a unit cell of masonry.

$$\omega^i = 0, \quad i = 1,4 \tag{18}$$

and

$$\underline{v}^1 = -\underline{v}^3 = \underline{\alpha}, \quad \underline{v}^2 = -\underline{v}^4 = \underline{\beta}. \tag{19}$$

By virtue of periodicity conditions, the velocity fields to be explored in the kinematic approach are thus completely defined by four parameters, namely the components of $\underline{\alpha}$ and $\underline{\beta}$. The corresponding macroscopic velocity gradient is given by

$$\underline{\underline{F}} = \frac{1}{ab}(2a\underline{\alpha} \otimes \underline{e}_1 + b\underline{\beta} \otimes \underline{e}_2) \tag{20a}$$

and

$$\underline{\underline{D}} = \frac{1}{b}(\underline{\alpha} \otimes^S \underline{e}_1) + \frac{1}{2a}(\underline{\beta} \otimes^S \underline{e}_2)\dagger, \tag{20b}$$

where a and b represent the height and the width of a block, respectively.

4.2. *Implementation of the kinematic approach*

Considering any velocity field of the above-described form, the virtual work of external forces corresponding to a prescribed value of $\underline{\underline{\Sigma}}$ becomes

$$\underline{\underline{\Sigma}} : \underline{\underline{D}} = \underline{\underline{\Sigma}} : \underline{\underline{F}} = \frac{1}{ab}[2a\alpha_1\Sigma_{11} + (2a\alpha_2 + b\beta_1)\Sigma_{12} + b\beta_2\Sigma_{22}]. \tag{21}$$

On the other hand the maximum resisting work given by formula (15) is

$$\langle \pi(\underline{\underline{d}}) \rangle = \frac{1}{ab}\int_J \tilde{\pi}(\underline{n}; [\underline{v}])\, \mathrm{d}J \tag{22}$$

since $\underline{\underline{d}} = \underline{\underline{0}}$ outside J with, for a Mohr–Coulomb strength condition such as (16) (see for instance Salençon, 1990),

$$\tilde{\pi}(\underline{n}; [\underline{v}]) = \begin{cases} (c/\tan\varphi)[\underline{v}] \cdot n & \text{if } [\underline{v}] \cdot n \geqslant |[\underline{v}]| \sin\varphi \\ +\infty & \text{otherwise} \end{cases}. \tag{23}$$

As shown by the above formula, the relevant velocity fields are subject to conditions concerning the velocity jumps across the joints. Taking the example of the vertical joint separating blocks 1 and 3, the discontinuity of velocity between these two blocks is equal to $2\underline{\alpha}$ (for $\underline{n} = \underline{e}_1$) so that (23) becomes

$$\tilde{\pi}(\underline{e}_1; 2\underline{\alpha}) = \begin{cases} (c/\tan\varphi)2\alpha_1 & \text{if } \alpha_1 \geqslant |\alpha_2| \tan\varphi \\ +\infty & \text{otherwise} \end{cases}. \tag{24a}$$

Analogous conditions relating to the velocity jumps $\underline{\beta} - \underline{\alpha}$ between blocks 2 and 1, and $\underline{\beta} + \underline{\alpha}$ between blocks 2 and 3 are

† $\underline{a} \otimes^S \underline{b} = 1/2(\underline{a} \otimes \underline{b} + \underline{b} \otimes \underline{a})$.

$$\beta_2 - \alpha_2 \geqslant |\beta_1 - \alpha_1| \tan\varphi, \tag{24b}$$

$$\beta_2 + \alpha_2 \geqslant |\beta_1 + \alpha_1| \tan\varphi. \tag{24c}$$

The corresponding value of the maximum resisting work (22) is

$$\langle \pi(\underline{\underline{d}}) \rangle = \frac{1}{ab} \frac{c}{\tan\varphi} (2a\alpha_1 + b\beta_2) \tag{25a}$$

and by means of (10) and (20b), it simply results that

$$\pi^{\text{hom}}(\underline{\underline{D}}) = (c/\tan\varphi)\,\text{tr}(\underline{\underline{D}}). \tag{25b}$$

It follows from the kinematic definition of G^{hom} expressed by (8), (10), (21) and (25) that G^{hom} is made of all the stress states $\underline{\underline{\Sigma}}$ such that

$$m\alpha_1\Sigma_{11} + (m\alpha_2 + \beta_1)\Sigma_{12} + \beta_2\Sigma_{22} \leqslant (c/\tan\varphi)(m\alpha_1 + \beta_2), \tag{26a}$$

where $m = 2a/b$, or

$$\underline{\underline{\Sigma}} : \underline{\underline{D}} \leqslant (c/\tan\varphi)\,\text{tr}(\underline{\underline{D}}) \tag{26b}$$

for any α_1, α_2, β_1 and β_2 satisfying conditions (24).

It can be shown (see Appendix for the demonstration) that G^{hom} is a convex polyhedral cone of vertex ($\Sigma_{11} = \Sigma_{22} = c/f, f = \tan\varphi, \Sigma_{12} = 0$) and such that the edges originating from this vertex are parallel to the following vectors:

$$\left\{\begin{matrix}-1\\0\\0\end{matrix}\right\}, \left\{\begin{matrix}f\\0\\-m\end{matrix}\right\}, \left\{\begin{matrix}-f\\\pm 1\\-1/f\end{matrix}\right\} \quad \text{if } m \leqslant 1/f,$$

$$\left\{\begin{matrix}-1\\0\\0\end{matrix}\right\}, \left\{\begin{matrix}f\\0\\-m\end{matrix}\right\}, \left\{\begin{matrix}-1/m\\\pm 1\\-m\end{matrix}\right\}, \left\{\begin{matrix}(-m-f+1/f)/mf\\\pm 1\\-1/f\end{matrix}\right\} \quad \text{if } m > 1/f.$$

Figure 5(a) and (b) represent the corresponding domain drawn in the space of stresses. Its boundary surface is made up of either four ($m \leqslant 1/f$) or six ($m > 1/f$) facets. The inherent anisotropy of the homogenized material is clearly evidenced from this geometrical representation, the uniaxial tensile strength, for instance, taking different values in the horizontal and vertical directions.

Comments.

• The above results link up with those obtained by Alpa and Monetto (1994) in the particular case of "dry block" masonry, that is when the cohesion c of the joint interfaces vanishes to zero. Actually, taking such a cohesion into account, simply amounts to performing a translation of vector $(c/\tan\varphi, 0, c/\tan\varphi)$ in the space of stresses. Unlike the work of Alpa and Monetto, which relies upon somewhat heuristic arguments, the present approach has been developed in a fully rigorous mechanical framework, constituted by the yield design homogenization method. Furthermore, it provides an irreplaceable means for extending the analysis to any kind of interface

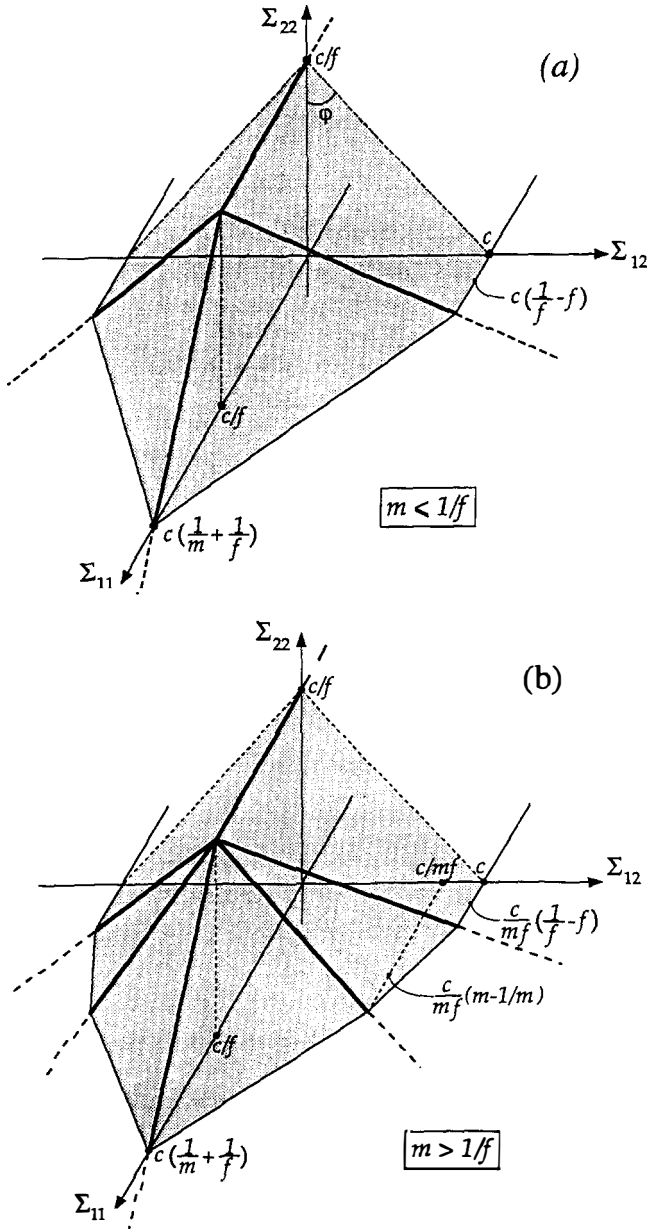

Fig. 5. Strength domain of brick masonry as a homogenized material in the space of stresses.

failure condition, as well as to taking into account limited strength capacities for the brick material.

• A quite simple upper bound approximation of the failure criterion may be deduced in the general case where the assumption of infinite resistance for the bricks appears to be unrealistic, so that failure of the masonry material as a whole is not exclusively

controlled by the joints. Indeed, it can be shown by exploiting the kinematic definition expressed by (10), where $\underline{u}$ represents a periodic velocity field combining discontinuities along the joints with deformation of the brick material itself, that the following relationship applies:

$$G_b^{hom} \subseteq G_\infty^{hom} \cap G^b,$$

where G_b^{hom} and G_∞^{hom} denote the strength domains corresponding to the limited and unlimited strength assumptions for the bricks, respectively. It follows that the resulting estimate is simply the intersection of the above constructed polyhedral domain shown in Fig. 5 with the brick strength domain. Whether such an estimate represents the exact failure condition remains yet to be proved.

5. APPLICATION TO STABILITY OF LATERALLY LOADED WALL SPECIMENS

The theoretical results obtained in the previous section will now be applied to the evaluation of the stability of block masonry walls submitted to a constant vertical specific weight γ, while the horizontal component of the body forces, denoted by $\lambda\gamma$, where $\lambda \geqslant 0$ is a non-dimensional loading parameter, is gradually increased. Such a problem has already been widely studied in order to investigate the mechanical response of masonry structures under seismic loading.

5.1. *Theoretical analysis*

An upper-bound estimate for the extreme value of λ is achieved through the yield design kinematic approach implemented on the homogenized structure. Referring to Fig. 6, a rigid block failure mechanism will be considered in which the part of the structure (denoted by B) which is located above the inclined line OO' is given a virtual rigid body motion defined by

$$\underline{v}(\underline{y}) = \underline{\chi} - \omega \underline{e}_3 \wedge \underline{y}, \tag{27}$$

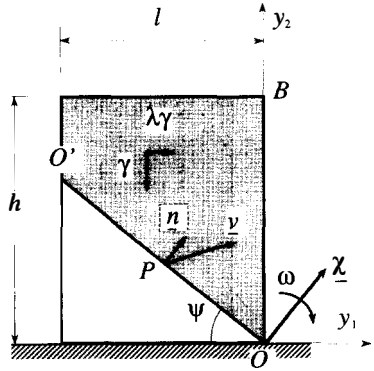

Fig. 6. Rigid block failure mechanism of homogenized masonry wall.

where ω is the angular velocity and $\underline{\chi}$ the velocity of point O, taken as the origin of a coordinate system (Oy_1y_2).

The work of the external forces [namely the uniform distribution of body forces $\gamma(\lambda \underline{e}_1 - \underline{e}_2)$] in such a mechanism is written

$$W_E = \gamma \int_B (\lambda \underline{e}_1 - \underline{e}_2) \cdot (\underline{\chi} + \underline{y} \wedge \pi \underline{e}_3) \, dy_1 \, dy_2, \tag{28}$$

or equivalently,

$$W_E = \gamma |B| (\lambda \chi_1 - \chi_2) + \omega M_0, \tag{29}$$

where $|B|$ is the area of the rotating block and M_0 represents the moment calculated about the Oy_3-axis of the body forces acting on B. Its expression is:

$$M_0 = \int_B (\lambda y_2 + y_1) \, dy_1 \, dy_2. \tag{30}$$

(Note that it is clockwise positive.)

It finally results that

$$W_E = A_1(\psi, \omega, \underline{\chi}) \lambda - A_2(\psi, \omega, \underline{\chi}), \tag{31}$$

where functions A_i have different expressions depending on the position of O':

- $\tan\psi \geqslant h/l$ (O' is located on the upper edge of the wall):

$$A_1 = \frac{\gamma h^2}{6 \tan\psi} (3\chi_1 + 2h\omega); \quad A_2 = \frac{\gamma h^2}{6 \tan\psi} (3\chi_2 + h\omega / \tan\psi), \tag{32a}$$

- $\tan\psi < h/l$ (O' is on the vertical edge of the wall):

$$A_1 = \frac{\gamma l}{6} [3(2h - l\tan\psi)\chi_1 + (3h^2 - l^2 \tan^2\psi)\omega],$$

$$A_2 = \frac{\gamma l}{6} [3(2h - l\tan\psi)\chi_2 + l(3h - 2l\tan\psi)\omega], \tag{32b}$$

where l and h denote the width and the height of the wall, respectively.

On the other hand, since no deformation occurs outside the discontinuity line OO', the maximum resisting work W_{MR} computed in such a mechanism reduces to:

$$W_{MR} = \int_{OO'} \tilde{\pi}^{hom}(\underline{n}, \underline{V}) \, ds, \tag{33}$$

where

$$\tilde{\pi}^{hom}(\underline{n}, \underline{V}) = \pi^{hom}(\underline{n} \otimes^S \underline{V}),$$

$\underline{V}$ being the velocity jump at any point P of OO' when crossing OO' following its normal $\underline{n}$. It follows from (25b) that

$$\tilde{\pi}^{\text{hom}}(\underline{n}, \underline{V}) = (c/\tan\varphi)(\underline{V} \cdot \underline{n}) \tag{34}$$

provided that the velocity jump $\underline{V}$ fulfills the following conditions derived from (A.5) and (A.8) where $\underline{D}$ is to be replaced by $\underline{n} \otimes^S \underline{V}$:

$$-v_1 n_1 \leqslant 0, \tag{35a}$$

$$\tan\varphi v_1 n_1 - m v_2 n_2 \leqslant 0 \tag{35b}$$

and either

$$|v_1 n_2 + v_2 n_1| \leqslant \tan\varphi v_1 n_1 + \frac{1}{\tan\varphi} v_2 n_2 \tag{35c}$$

if $m \leqslant 1/\tan\varphi$, or

$$|v_1 n_2 + v_2 n_1| \leqslant \frac{1}{m} v_1 n_1 - m v_2 n_2 \tag{35d}$$

and

$$|v_1 n_2 + v_2 n_1| \leqslant \frac{1}{\tan\varphi}\left[\frac{1}{m}\left(m + \tan\varphi - \frac{1}{\tan\varphi}\right) v_1 n_1 + v_2 n_2\right] \tag{35e}$$

in the case when $m > 1/\tan\varphi$.

Since the velocity jump at any point P is $\underline{V}(P) = \underline{\chi} - \omega \underline{e}_3 \wedge \underline{OP}$, it follows that

$$W_{\text{MR}} = cL(\chi_1 \sin\psi + \chi_2 \cos\psi + \omega L/2)/\tan\varphi, \tag{36}$$

where L denotes the length of the discontinuity line OO', and where parameters $\psi, \underline{\chi}$ and ω are subject to a set of linear constraints which can be deduced from conditions (35).

The yield design upper-bound theorem states that, for the structure to be safe under a given load factor λ, it is necessary that the work of the corresponding external forces in any kinematically admissible failure mechanism remains lower than or equal to the maximum resisting work:

$$W_{\text{E}} = \lambda A_1 - A_2 \leqslant W_{\text{MR}}$$

and then for $A_1 > 0$,

$$\lambda^* \leqslant \min_{(\psi, \omega, \underline{\chi})} \left\{\frac{W_{\text{MR}} + A_2}{A_1}\right\} = \lambda^+, \tag{37}$$

where λ^* denotes the ultimate value of λ. It thus appears that, minimizing the right hand member of (37) with respect to parameters ψ, $\underline{\chi}$ and ω subject to the above-mentioned linear constraints, results in deriving an upper-bound value for λ^*.

5.2. *Analytical results for dry block masonry and comparison with experiments*

In the case of dry block masonry, where the joints exhibit purely frictional strength properties ($c = 0$), it can be easily seen from dimensional analysis arguments that

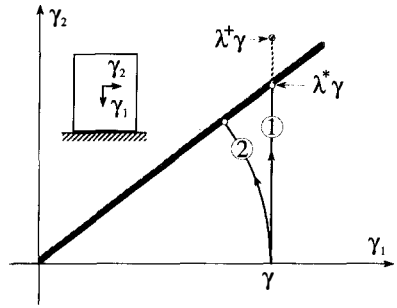

Fig. 7. Stability domain of dry block masonry rectangular wall in the plane of load parameters (γ_1, γ_2).

the extreme value λ^* of the loading parameter is a function of the sole following dimensionless variables: m, φ and $\rho = h/l$, noting in particular that it does not depend on the specific weight γ. Therefore the stability domain of the structure, drawn in the quarter-plane ($\gamma_1 = \gamma \geqslant 0, \gamma_2 = \lambda\gamma \geqslant 0$) is simply bounded by the semi-line of equation $\gamma_2 = \lambda^*\gamma_1$ (Fig. 7) and the yield design kinematic approach described in the previous section leads to the determination of an upper bound value $\gamma_2 = \lambda^+\gamma_1$ located on the vertical loading path No. 1 defined by $\gamma_2 = \lambda\gamma$.

Simple analytical expressions for λ^+ can be obtained by considering rigid translation ($\omega = 0$) and rigid rotation about O ($\underline{\chi} = 0$) separately. For a rigid body translation depending on ψ and $\underline{\chi}$, (37) becomes

$$\lambda^* \leqslant \lambda^+ = \min_{(\psi, \underline{\chi})} \left\{ \frac{A_2(\psi, \underline{\chi})}{A_1(\psi, \underline{\chi})} \right\} \tag{38}$$

since the maximum resisting work given by (34) vanishes to zero for any corresponding mechanism satisfying conditions (35). The optimization finally yields

$$\lambda^* \leqslant \lambda^+ = \tan\varphi. \tag{39}$$

Likewise, for a rigid body rotation about point O ($\underline{\chi} = 0$), conditions (35) reduce to $\tan\psi \leqslant (m/\tan\varphi)^{1/2}$ and the best upper-bound estimate produced by this particular class of mechanisms is:

$$\lambda^* \leqslant \lambda^+ = \begin{cases} \frac{1}{2}(m/\tan\varphi)^{1/2} & \text{if } \rho = h/l \leqslant (m/\tan\varphi)^{1/2} \\ \dfrac{3\rho - 2(m/\tan\varphi)^{1/2}}{3\rho^2 - (m/\tan\varphi)} & \text{otherwise.} \end{cases} \tag{40}$$

As could have been anticipated from dimensional analysis arguments, those estimates depend only on ρ, m and φ. They can be compared with experimental values obtained from tests carried out at the *Ingegneria Strutturale e Geotecnica* department of the University of Rome on model walls, brought to failure by tilting the plane supporting the structure. This is equivalent to inclining the gravity by an angle θ with respect to the Oy_1y_2 axes, thus following, in the plane of load parameters (γ_1, γ_2), a circular loading path (path No. 2 in Fig. 7) defined by

$$\gamma_1 = \gamma\cos\theta, \quad \gamma_2 = \gamma\sin\theta. \tag{41}$$

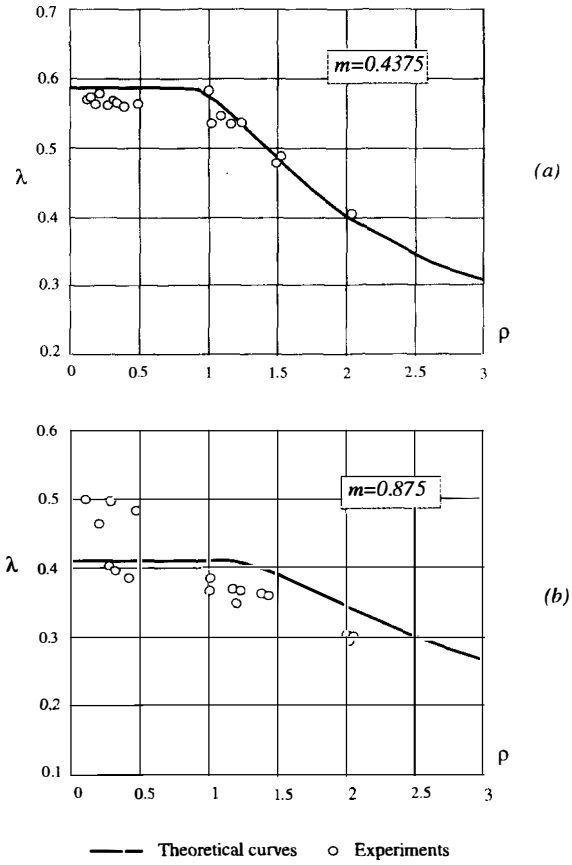

Fig. 8. Theoretical estimates versus experimental data concerning the limit load of laterally loaded block masonry walls.

The values of $\lambda^{exp} = \tan(\theta^{lim})$, where θ^{lim} represents the limit tilting angle at which breakage of the wall specimen has been observed, have been plotted in Fig. 8 displaying the variations of the theoretical estimates λ^{+} given by formulas (39) and (40) as a function of ρ and m, for a value of the joint friction angle equal to 31° ($\tan\varphi = 0.6$).

6. DISCUSSION AND CONCLUDING REMARKS

Several comments should first be made relating to Fig. 8(a) and (b). In accordance with intuition, both experimental and theoretical results show that the stability of the structure is a decreasing function of its slenderness, characterized by the dimensionless factor $\rho = h/l$. Likewise, those results clearly demonstrate that taking bricks with the smaller aspect ratio considerably improves the stability.

Focusing on the comparison between experimental data and theoretical predictions, one can observe quite good agreement between them for $m = 0.4375$, since it should be kept in mind that calculated values are upper-bound estimates for the exact limit

loads. On the other hand there is a significant discrepancy between the theoretical curve and the experimental points for $m = 0.875$. For small slenderness ratios, in particular $\rho = 0.5$, the experimental limit loads are greater than those predicted by the theoretical analysis.

The following argument may be put forward as a possible explanation for such a difference. Indeed, it is to be remembered that the validity of the yield design homogenization method, as it has been applied in this paper, is strongly dependent on the fact that the characteristic length of the heterogeneity (here the size of the elementary bricks) remains sufficiently smaller than the overall dimensions of the structure, such as, for example, the height of the wall.

More precisely, the following convergence result has been established (Suquet, 1983; de Buhan, 1986):

$$\lim_{\varepsilon \to 0} Q^{\varepsilon} = Q^{\hom}, \tag{42}$$

where ε denotes a small non-dimensional parameter standing for the ratio between the dimension of the unit cell and that of the whole structure, while Q^{ε} and $Q^{\hom}$ denote the limit loads of the initial structure and the homogenized structure, respectively.

Furthermore, as regards the problem under consideration, it turns out that some experiments were carried out on specimens comprising relatively few layers of bricks, which corresponds to an insufficiently small value of the parameter ε, so that the applicability of the homogenization method appears questionable in these cases.

Therefore, it is clear that such a difference between theory and experience is to be attributed to a "scale" or "size effect" which is not included in the theoretical model. It can be overcome by resorting to a description of masonry as a micropolar or Cosserat continuum, as proposed by Besdo (1985) and more recently by Masiani and Trovalusci (1995) or Masiani *et al.* (1995) in the context of an elastic behaviour for modelling the interactions between bricks. Indeed, this kind of model can account for interacting couples between blocks through couple-stresses, and thus provide a more realistic description than the classical continuum theory. A quite interesting line of research for the future would be to demonstrate how such models could be derived from a possible generalization of the homogenization theory for periodic media. However, owing to the fact that the above-mentioned "scale effect" is considerably accentuated by the constitutive rigidity of the bricks, it could be expected that such a question will not have the same importance for a brick material exhibiting limited strength properties.

ACKNOWLEDGEMENT

Financial support has been provided to G. de Felice by the European Community's program "Human Capital and Mobility".

REFERENCES

Alpa, G. and Monetto, I. (1994) Microstructural model for dry block masonry walls with in-plane loading. *J. Mech. Phys. Solids* **42**(7), 1159–1175.

Anthoine, A. (1995) Derivation of the in-plane elastic characteristics of masonry through homogenization theory. *Int. J. Solids Struct.* **32**(2), 137–163.
Baggio, C. and Trovalusci, P. (1993) Discrete models for jointed block masonry walls. *Proc. 6th North American Masonry Conf.*, Philadelphia, Pennsylvania, pp. 939–949.
Bekaert, A. and Maghous, S. (1996) Three dimensional yield strength properties of jointed rockmass as a homogenized medium. *Int. J. Cohesive Frictional Mater.* **1**, 1–24.
Besdo, D. (1985) Inelastic behaviour of plane frictionless block-systems described as Cosserat media. *Arch. Mech.* **37**(6), 603–619.
Cundall, P. A. (1971) A computer model for simulating progressive large-scale movements in block rock systems. *Proc. Int. Symp. Rock Fracture*, Nancy, France, II-8.
de Buhan, P. (1986) Approche fondamentale du calcul à la rupture des ouvrages en sols renforcés. Thèse d'Etat, Université de Paris-VI.
de Buhan, P. and Salençon, J. (1990) Yield strength of reinforced soils as anisotropic media. In *Mechanical Engineering Publications*, ed. J. P. Boehler, pp. 791 803. Mech. Eng. Publ., London.
de Buhan, P. and Taliercio, A. (1991) A homogenization approach to the yield strength of composite materials. *Eur. J. Mech. A/Solids* **10**(2), 129–154.
de Felice, G. (1994) Omogeneizzazione e calcolo a rottura della muratura. *Tesi di dottorato*. Dip. Ingegneria Strutturale e Geotecnica, Roma.
Frémond, M. and Friaà, A. (1982) Les méthodes statique et cinématique en calcul à la rupture et analyse limite. *J. Mech. Th. Appl.* **5**, 881–905.
Giuffrè, A., Pagnoni, T. and Tocci, C. (1994) In-plane seismic behaviour of historical masonry walls. *Proc. 10th Int. Brick/Block Masonry Conf.*, Calgary, Canada.
Heyman, J. (1966) The Stone Skeleton, *Int. J. Solids Structures* **2**, 249–279.
Livesley, R. K. (1978) Limit analysis of structures formed from rigid blocks. *Int. J. Numer. Methods Engng* **12**, 1853–1871.
Lofti, H. R. and Shing, P. B. (1994) Interface model applied to fracture of masonry structures. *J. Struct. Engng ASCE*, **120**(1), 63–80.
Maier, G., Nappi, A. and Papa, E. (1991) On damage and failure of brick masonry. In *Experimental and Numerical Methods in Earthquake Engineering*, J. Donea and P. M. Jones, pp. 223–245. The Netherlands.
Masiani, R. and Trovalusci, P. (1995) Size effects in continuum modeling of brick masonry. *Computer Methods in Structural Masonry—3*, ed. J. Middleton and G. N. Pande, pp. 42–51. Books and Journals International Ltd.
Masiani, R., Rizzi, N. and Trovalusci, P. (1995) Masonry as structured continuum. *Meccanica* **30**, 673–683.
Page, A. W. (1978) Finite element model for masonry. *J. Struct. Engng ASCE*, **104**(8), 1267–1285.
Pande, G. N., Liang, J. X. and Middleton, J. (1989) Equivalent elastic moduli for brick masonry. *Comput. Geotech.* **8**, 243–265.
Pietruszczak, S. and Niu, X. (1992) A mathematical description of macroscopic behaviour of brick masonry. *Int. J. Solids Struct.* **29**(5), 531–546.
Salençon, J. (1990) An introduction to the yield design theory and its application to soil mechanics. *Eur. J. Mech. A/Solids* **9**(5), 477–550.
Salençon, J. (1992) Yield design : a survey of the theory. In : *CISM Courses and Lectures*, 332, pp. 1–44. Springer-Verlag, Wien, New York.
Suquet, P. (1983) Analyse limite et homogénéisation. *C.R. Acad. Sci., Paris* **296** (série II), 1355 1358.

APPENDIX : DETERMINATION OF G^{hom} IN THE SPACE OF STRESSES

We start from the kinematic definition (26) where parameters α_i and β_i are subject to conditions (24). Let

$$D_{11} = \frac{2}{b}\alpha_{11}, \quad D_{12} = \frac{1}{b}\alpha_2 + \frac{1}{2a}\beta_1, \quad D_{22} = \frac{1}{\alpha}\beta_2 \tag{A.1}$$

and

$$\Sigma'_{11} = \Sigma_{11} - c/f, \quad \Sigma'_{12} = \Sigma_{12}, \quad \Sigma'_{22} = \Sigma_{22} - c/f \tag{A.2}$$

be, respectively, the components of $\underline{\underline{D}}$ and $\underline{\underline{\Sigma}}' = \underline{\underline{\Sigma}} - (c/\tan\varphi)\,\underline{\underline{I}}$ in the reference of the joint directions of masonry texture, where $f = \tan\varphi$. Inequality (26) may be rewritten as:

$$\Sigma'_{11}D_{11} + 2\Sigma'_{12}D_{12} + \Sigma'_{22}D_{22} \leqslant 0 \tag{A.3}$$

with conditions (24) becoming

$$\begin{aligned}
&-\frac{b}{2f}D_{11} \leqslant \alpha_2 \leqslant \frac{b}{2f}D_{11},\\
&\frac{b}{2}D_{11} + 2\alpha D_{12} - \frac{a}{f}D_{22} \leqslant \alpha_2\left(\frac{2a}{b} + \frac{1}{f}\right) \leqslant -\frac{b}{2}D_{11} + 2aD_{12} + \frac{a}{f}D_{22},\\
&-\frac{b}{2}D_{11} + 2aD_{12} - \frac{a}{f}D_{22} \leqslant \alpha_2\left(\frac{2a}{b} - \frac{1}{f}\right) \leqslant \frac{b}{2}D_{11} + 2aD_{12} + \frac{a}{f}D_{22},
\end{aligned} \tag{A.4}$$

where the parameter α_2 remains arbitrary.

Two cases should then be considered according to the sign of $(2(a/b) - (1/f))$:

- $0 < 2a/b < 1/f$. The set of constraints (A.4) can be rearranged into

$$\begin{aligned}
&-\frac{b}{2f}D_{11} \leqslant \alpha_2 \leqslant \frac{b}{2f}D_{11},\\
&\left(\frac{1}{f} + \frac{2a}{b}\right)^{-1}\left(\frac{b}{2}D_{11} + 2aD_{12} - \frac{a}{f}D_{22}\right) \leqslant \alpha_2 \leqslant \left(\frac{1}{f} + \frac{2a}{b}\right)^{-1}\left(-\frac{b}{2}D_{11} + 2aD_{12} + \frac{a}{f}D_{22}\right),\\
&\left(\frac{1}{f} - \frac{2a}{b}\right)^{-1}\left(-\frac{b}{2}D_{11} - 2aD_{12} - \frac{a}{f}D_{22}\right) \leqslant \alpha_2 \leqslant \left(\frac{1}{f} - \frac{2a}{b}\right)^{-1}\left(\frac{b}{2}D_{11} - 2aD_{12} + \frac{a}{f}D_{22}\right).
\end{aligned}$$

The existence of a solution for α_2 requires that all upper bounds of the above inequalities be greater than or equal to the lower bounds, that is after having eliminated the redundant inequalities:

$$\begin{aligned}
g^{(1)}(D_{11}, D_{12}, D_{22}) &= -D_{11} \leqslant 0,\\
g^{(2)}(D_{11}, D_{12}, D_{22}) &= fD_{11} - mD_{22} \leqslant 0,\\
g^{(3)}(D_{11}, D_{12}, D_{22}) &= -fD_{11} + 2D_{12} - \frac{1}{f}D_{22} \leqslant 0,\\
g^{(4)}(D_{11}, D_{12}, D_{22}) &= -fD_{11} - 2D_{12} - \frac{1}{f}D_{22} \leqslant 0.
\end{aligned} \tag{A.5}$$

The set of $\underline{A} = (D_{11}, D_{12}, D_{22})$ defined by the conditions (A.5) is a convex cone bounded by planes of equations $g^{(k)}(D_{11}, D_{12}, D_{22}) = 0$, $k = 1$ to 4, so that the set of $\underline{X} = (\Sigma'_{11}, \Sigma'_{12}, \Sigma'_{22})$ characterized by (A.3) is also a polyhedral cone formed by all the convex combinations of the normal to those planes:

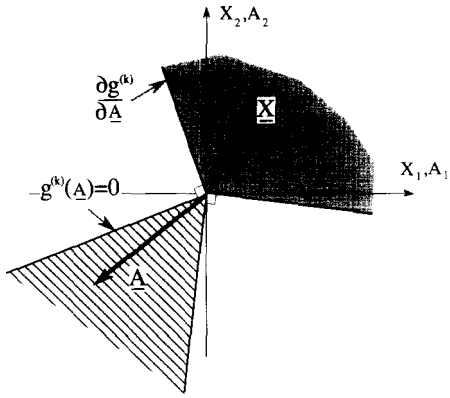

Fig. 9. Convex cones of admissible $\underline{A}$ and $\underline{X}$.

$$\underline{X} = \sum_{k=1}^{4} \lambda_k \frac{\partial g^{(k)}}{\partial \underline{A}}, \quad \lambda_k \geqslant 0. \tag{A.6}$$

Figure 9, drawn in R^2 for the sake of simplicity, represents those convex cones. It follows that

$$\underline{X} = \lambda_1 \begin{pmatrix} -1 \\ 0 \\ 0 \end{pmatrix} + \lambda_2 \begin{pmatrix} f \\ 0 \\ -m \end{pmatrix} + \lambda_3 \begin{pmatrix} -f \\ 1 \\ -1/f \end{pmatrix} + \lambda_4 \begin{pmatrix} -f \\ -1 \\ -1/f \end{pmatrix} \tag{A.7}$$

with $\lambda_{1,4} \geqslant 0$. Hence the corresponding domain in the space of stresses $(\Sigma_{11}, \Sigma_{12}, \Sigma_{22})$ in Fig. 5(a).

• $2a/b > 1/f$. The demonstration is quite similar to that of the previous case. The set of constraints (A.4) is transformed into

$$-\frac{b}{2f} D_{11} \leqslant \alpha_2 \leqslant \frac{b}{2f} D_{11},$$

$$\left(\frac{2a}{b} + \frac{1}{f}\right)^{-1} \left(\frac{b}{2} D_{11} + 2aD_{12} - \frac{a}{f} D_{22}\right) \leqslant \alpha_2 \leqslant \left(\frac{2a}{b} + \frac{1}{f}\right)^{-1} \left(-\frac{b}{2} D_{11} + 2aD_{12} + \frac{a}{f} D_{22}\right),$$

$$\left(\frac{2a}{b} - \frac{1}{f}\right)^{-1} \left(-\frac{b}{2} D_{11} + 2aD_{12} - \frac{a}{f} D_{22}\right) \leqslant \alpha_2 \leqslant \left(\frac{2a}{b} - \frac{1}{f}\right)^{-1} \left(\frac{b}{2} D_{11} + 2aD_{12} + \frac{a}{f} D_{22}\right).$$

A solution for α_2 is ensured if and only if the following inequalities involving D_{11}, D_{12} and D_{22} are satisfied:

$$h^{(1)}(D_{11}, D_{12}, D_{22}) = -D_{11} \leqslant 0,$$

$$h^{(2)}(D_{11}, D_{12}, D_{22}) = fD_{11} - mD_{22} \leqslant 0,$$

$$h^{(3)}(D_{11}, D_{12}, D_{22}) = -\frac{1}{m} D_{11} + 2D_{12} - mD_{22} \leqslant 0,$$

$$h^{(4)}(D_{11}, D_{12}, D_{22}) = -\frac{1}{m} D_{11} - 2D_{12} - mD_{22} \leqslant 0,$$

$$h^{(5)}(D_{11}, D_{12}, D_{22}) = -\frac{1}{mf}\left(m - \frac{1}{f} + f\right) D_{11} + 2D_{12} - \frac{1}{f} D_{22} \leqslant 0,$$

$$h^{(6)}(D_{11}, D_{12}, D_{22}) = -\frac{1}{mf}\left(m - \frac{1}{f} + f\right) D_{11} - 2D_{12} - \frac{1}{f} D_{22} \leqslant 0, \tag{A.8}$$

so that the set of admissible values of $\underline{X} = (\Sigma'_{11}, \Sigma'_{12}, \Sigma'_{22})$ is a polyhedral cone defined by

$$\underline{X} = \mu_1 \begin{pmatrix} -1 \\ 0 \\ 0 \end{pmatrix} + \mu_2 \begin{pmatrix} f \\ 0 \\ -m \end{pmatrix} + \mu_3 \begin{pmatrix} -1/m \\ 1 \\ -m \end{pmatrix} + \mu_4 \begin{pmatrix} -1/m \\ -1 \\ -m \end{pmatrix}$$

$$+ \mu_5 \begin{bmatrix} \frac{1}{mf}\left(\frac{1}{f} - m - f\right) \\ 1 \\ -1/f \end{bmatrix} + \mu_6 \begin{bmatrix} \frac{1}{mf}\left(\frac{1}{f} - m - f\right) \\ -1 \\ -1/f \end{bmatrix} \tag{A.9}$$

with $\mu_{1,6} \geqslant 0$. The corresponding domain in the space of stresses is sketched in Fig. 5(b).